Vol. 41, No. 3 (2019) 330-343, DOI: 10.24874/ti.2019.41.03.03

Tribology in Industry

www.tribology.rs

RESEARCH

Influence of the Number of Bilayers on the Mechanical and Tribological Properties in [TiN/TiCrN]n Multilayer Coatings Deposited by Magnetron Sputtering

C.H. Ortiz[a], H.D. Colorado[b], W. Aperador[c], A. Jurado[a]

[a] *School of Materials Engineering, Universidad del Valle, Cali, Colombia,*
[b] *Physics department , Universidad del Valle, Cali, Colombia,*
[c] *Universidad Militar Nueva Granada, Bogotá, Colombia.*

Keywords:

Magnetron sputtering
Coatings
Mechanical properties
Friction coefficient
Electrochemical properties

Corresponding author:

Christian Ortiz Ortiz
Escuela de ingeniería de materiales,
Universidad del Valle; Calle 13
No 100-00, Cali, Colombia,
E-mail:
Christian.ortiz.ortiz@correounivalle.edu.co

A B S T R A C T

In this work the influence of the number of bilayers was studied on the mechanical, tribological and electrochemical properties of multilayer coatings [TiN / TiCrN]n as a function of the number of bilayers n = 1, 25 and 50, deposited by magnetron sputtering. By X-ray diffraction (XRD), a cubic crystal structure centered on the faces (FCC) was determined for all coatings and an increase in the compressive stresses that were generated during the deposition process was found by perfilometry; Atomic force microscopy (AFM) determined that by increasing the number of bilayers, the roughness decreased, due to an increase in the density of the system. By nanoindentation it was found that the hardness (H) and the modulus of elasticity (E) increased as the number of bilayers did. By Pin on disk a decrease in the coefficient of friction was observed as the number of bilayers was increased, which was related to the increase in hardness and the reduction of roughness. The results of EIS and Tafel for the electrochemical properties, determined that the corrosion rate decreased due to the fact that a greater barrier to the passage of the electrolyte towards the substrate is promoted when the number of bilayers increases.

1. INTRODUCTION

The phenomena of friction and wear produce a large amount of losses within the manufacturing industry, generating higher costs within the production process, as well as negative effects on the productivity and competitiveness of these companies. [1]. The engineering of surfaces arises as a solution to this problem, more specifically surface treatments such as hard coatings, which are obtained by means of techniques such as PVD, CVD and others [2].

Hard coatings have been extensively studied for their contribution to improving surface properties of a variety of industrial devices such as cutting tools and injection molds [3]. In the literature you can find different coating systems based on nitrides and carbides such as TiN [4],[5], ZrN [5], TCN [6] , TiAlN [7], CrN [8] y ZrCN [9] which have good properties such as hardness, low friction coefficient and good resistance to corrosion, among other desirable properties. Consequently, in the current literature it is possible to observe numerous studies on binary coatings such as TiN, presenting very interesting results in properties such as hardness and wear resistance [5], and ternary coatings such as TiCrN which, in addition to presenting important properties such as hardness and wear resistance, has a high resistance to corrosion [3,10,11], by combining the two systems TiN and TiCrN to form a new multi-layer system [TiN/ TiCrN]n, a structure with better properties than each separate coating is produced. Multilayer coatings are known to have better mechanical, tribological and electrochemical properties compared to monolayer coatings because these nanometric periods allow a relaxation and dissipation of stresses as well as greater impediments to the movement of cracks, being this a better system for coating cutting tools by extending its service life [12,13].

Taking into account what is previously mentioned, no reports have been found on synergisms in the mechanical, tribological and electrochemical properties of multilayer coatings of the [TiN/TiCrN]n system, therefore the present work was carried out in order to provide knowledge on said coatings, and thus study is presents monolayer coatings (TiN and TiCrN) and multilayers [TiN/TiCrN]n as a function of the number of bilayers 1, 25 and 50. All monolayer and multilayer coatings have thicknesses of 1 μm. The mechanical, tribological and electrochemical properties were studied, correlating them with the morphology of all the coatings to determine which system had the best properties as a whole, which are of great potential in the application of coatings on tools for industrial use.

2. EXPERIMENTAL SECTION

The deposition was performed by means of the PVD technique using a non-reactive magnetron co-sputtering DC with an AJA international ATC 1500 equipment, in which titanium (Ti) targets with a purity of 99.99 % and a chromium target (Cr) with 99.99 % purity were used.

Seven samples of AISI H13 steel, four silicons (100) and one dinasyl were positioned in the substrate holder, which were placed symmetrically in order to obtain equal thicknesses on the surfaces. Before carrying out the deposition process, a plasma cleaning was carried out for both cathodes (Ti and Cr), with 100 V and 50 V respectively, in order to remove impurities (closed seals). After the plasma cleaning the deposition process of the coatings was performed with the variables shown in Table 1.

The thicknesses for all the monolayer and multilayer coatings were 1 μm, for the bilayers 1, 25 and 50 monolayer thicknesses of 50 nm, 20 nm and 10 nm were obtained, respectively. The crystalline structure was analyzed by means of X-ray diffraction using an X'Pert PRO MRD diffractometer from PANalytical. For this, the grazing incidence technique was used to allow the diffraction of the atomic planes perpendicular to the surface of the sample. The source of the x ray that was used was that of Cu kα, which had a wavelength of 1.5406 Å.

The chemical analysis was performed using a JEOL Model JSM 6490 LV microscope in the backscattered electron mode through an acceleration voltage of 20 kV. Additionally, chemical microanalyses were carried out on several inspection areas, using the EDS probe of the Oxford Instrument Model INCAPentaFETx3.The surface characterization for all the coatings was carried out with a MFP-3D equipment from Asylum Research in contact mode, the measurement of roughness and grain size were obtained over an area of 1 μm2, and the results were analyzed with the Scanning Probe Image Processor program (SPIP).

The mechanical properties (hardness, modulus of elasticity) were analyzed using a Nanovea nanoindentator, which uses a diamond tipped Berkovich indentor with a compliance of 0.00035 μm/mN. Corrections and results analysis were performed using Oliver's method and Pharr with indentations below 10 % of the coating thickness.

Tabla 1. Deposition parameters of the coatings.

Temperature (ºC)	Chamber Temperature
Base pressure (Torr)	$4x10^{-6}$
Working Pressure (Torr)	$3x10^{-3}$
Distance between electrodes (cm)	10 cm
Diameter of cathodes (cm)	5.08
Rotation speed of the substrate holder (rpm)	30
Gases used	Argon and Nitrogen
Argon flow	10.0 sccm
Nitrogen Flow	0.14 sccm
Pressure Sensors	Baratron convectron sensor for pressures from 750 Torr to $1x10^{-2}$ Torr, capacitive pressure gauge sensor for pressure ranges from $1x10^{-2}$ Torr to $1x10^{-4}$ Torr, ion gauge type sensor for pressures between $1x10^{-4}$ Torr to $1x10^{-11}$ Torr.
Power source	ATX 1500, range up to 25 W/cm^2
Cathode voltage Cr	50 V
Cathode voltage Ti	100 V
Source bias	Advanced energy range up to 1kV
Bias voltage	-100 V

The tribological characterization was performed with a CSEM Instruments tribometer following the ASTM G99-05 standard, a steel 440 counterpar was used and the test was carried out for 100 m with a constant load of 5 N. Subsequently, the analysis was completed using a scanning electron microscope (JEOL Model JSM-6480 LV), with which the wear track was observed to see the wear mechanisms produced during the test for all the systems.

The dynamic scratch analysis was determined based on the ASTM C1624-05 standard, using a NANOVEA M1 equipment with a coupling for dynamic scratching (scratch tester Nanoindentator) and the NANOVEA SCRATCH TESTER software. A Rockwell C indenter was used, with a diamond tip of 200 µm and a force of 0.01 N to 35 N. To analyze the electrochemical properties, the electrochemical impedance was first determined using a PC-14 model Gamry equipment, with a platinum counter electrode, an Ag / AgCl reference electrode and a sodium chloride (NaCl) electrolyte at 3.5 %. Subsequently, the tafel curves were performed using a PGTEKCORR 4.1 USB Potentiostat Galvanostat, with which the corrosion potential and the corrosion rate were determined using a graphite counter electrode, an Ag / AgCl reference electrode and a sodium chloride electrolyte (NaCl) at 3.5 %.

3. RESULTS

3.1 X- Ray Diffraction Analysis

Figure 1 shows the diffraction patterns for the monolayer and multilayer coatings as a function of the number of bilayers deposited on substrates of Si (100) where diffraction peaks were obtained located in the crystallographic planes (111) (200), (220) , (311), (222) and (400). From these results it was possible to infer that all coatings have a face-centered cubic crystal structure (FCC).

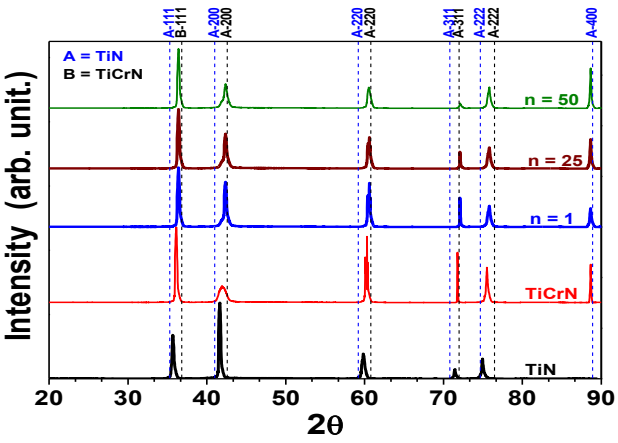

Fig. 1. X-ray diffraction patterns for monolayers [TiN and TiCrN] and multilayers [TiN/TiCrN]n as a function of the number of bilayers 1, 25, and 50.

The internal stresses produced during the deposition process, as well as the incorporation the chromium (Cr) into the structure of titanium nitride (TiN) in the coatings, caused a deformation between the crystalline planes, which generated a displacement in the diffraction peaks as illustrated in Fig. 1 [10], to analyse these stresses the variation in the lattice parameters was studied, which were calculated by means of Bragg's law Eq. (1) and the lattice parameter equation Eq. (2):

$$n\lambda = 2dsen\theta \quad (1)$$

$$d = \frac{\alpha_0}{\sqrt{h^2+k^2+l^2}} \quad (2)$$

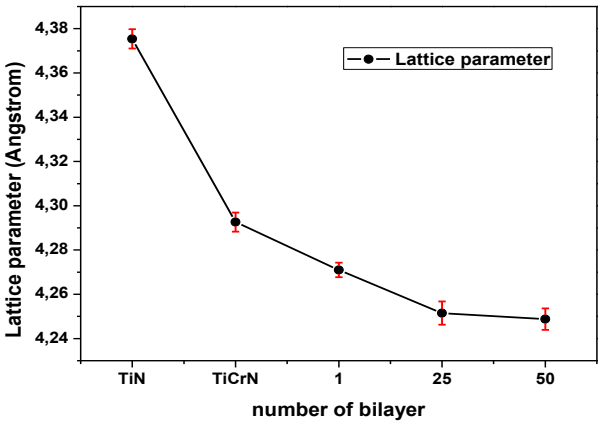

Fig 2. Lattice parameters for monolayer [TiN and TiCrN] and multilayer [TiN/TiCrN]n coatings as a function of the number of bilayers 1, 25 and 50.

Figure 2 shows the lattice parameters for all the coatings, where it could be seen that the (TiCrN) monolayer coating had a lattice parameter smaller than the (TiN) coating, this compressive type deformation was produced by the incorporation of the (Cr) within its structure [10]; In the multilayer coatings, this behaviour was more evidenced as the number of interfaces increased, since a greater compressive type deformation was generated in the crystalline structure, therefore, it was determined that the coating with 50 bilayers showed a greater compressive type deformation in the crystalline structure.

3.2 Chemical Analysis.

With the results obtained by means of chemical analysis (EDS) on the spectra shown in Figure 3 for the monolayer and multilayer coatings, Table 2 was made. This expresses the percentage by weight of each element present, where it was corroborated that the bilayers 1, 25 and 50 did not present a considerable variation in the chemical composition, demonstrating that the change of the mechanical, tribological and electrochemical properties were due solely to a change of physical order by a variation in the number of bilayers.

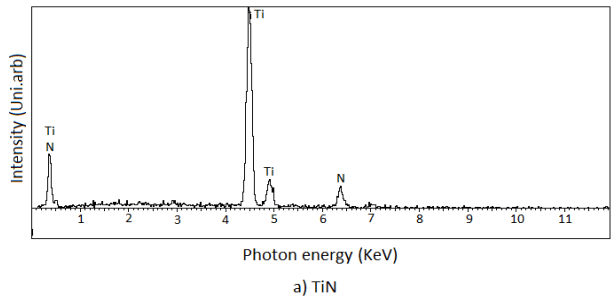

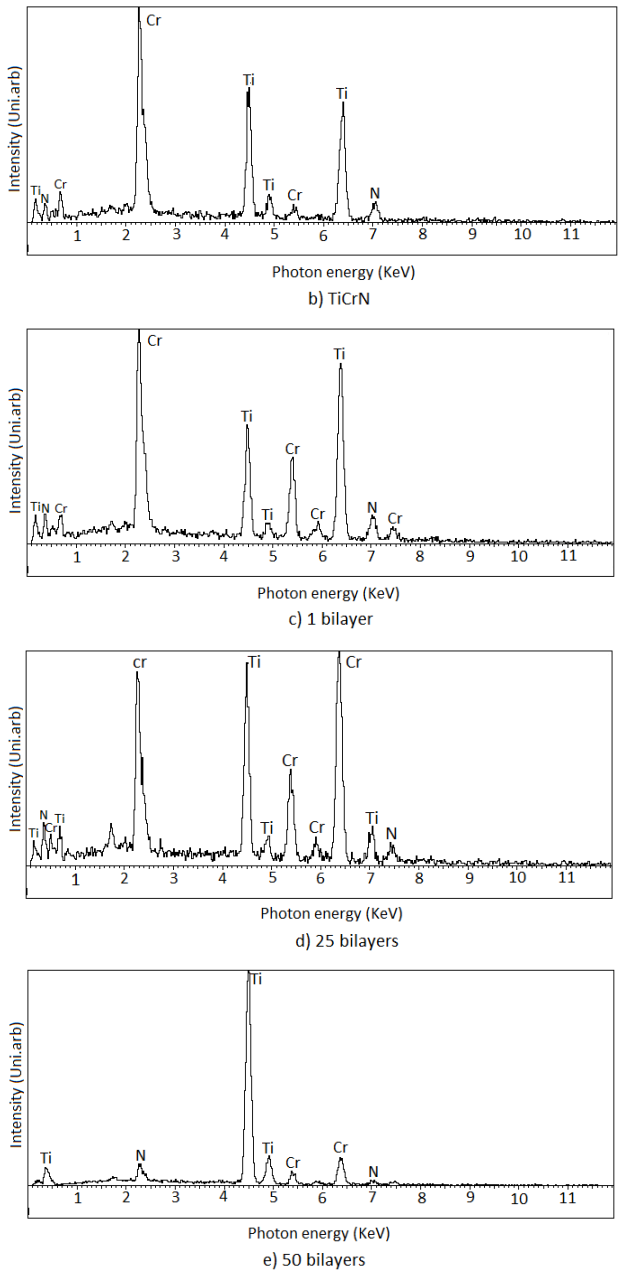

Fig. 3. Chemical analysis for a) TiN b) TiCrN c) 1 bilayer d) 25 bilayers and e) 50 bilayer.

Table 2. Chemical composition for monolayer and multilayer coatings.

Monolayer	% Porcentage by weight		
	Ti	Cr	N
TiN	69.90 ± 2.07	0	30.00± 2.10
TiCrN	29.00 ± 0.87	23.37± 1.62	36.70± 2.56
1 bilayer	33.20 ± 0.99	32.64± 2.28	34.13± 2.38
25 bilayer	35.68 ± 1.07	33.50± 2.48	30.80± 2.01
50 bilayer	36.12 ± 1.08	30.42± 2.12	33.46± 2.34

3.3 Surface Analysis.

To study the surface morphology of the samples quantitatively, the atomic force microscopy (AFM) technique was used. Figures 4a and 4b represent

the images for monolayers of titanium nitride (TiN) and titanium chromium nitride (TiCrN), respectively, where it is possible to demonstrate that the surface of TiCrN has a more regular surface; This change in the surface is due to the incorporation of chromium (Cr) in its crystalline structure, which causes a greater compressive type deformation as corroborated previously in Fig. 2, making a much more compact structure with a more orderly growth. Figures 4c, 4d and 4e show the images for bilayers n = 1, 25 and 50 respectively, where it is evidenced, that when increasing the number of bilayers or interfaces, the surface has a smaller number of imperfections because the system becomes much denser generating a more regular surface.

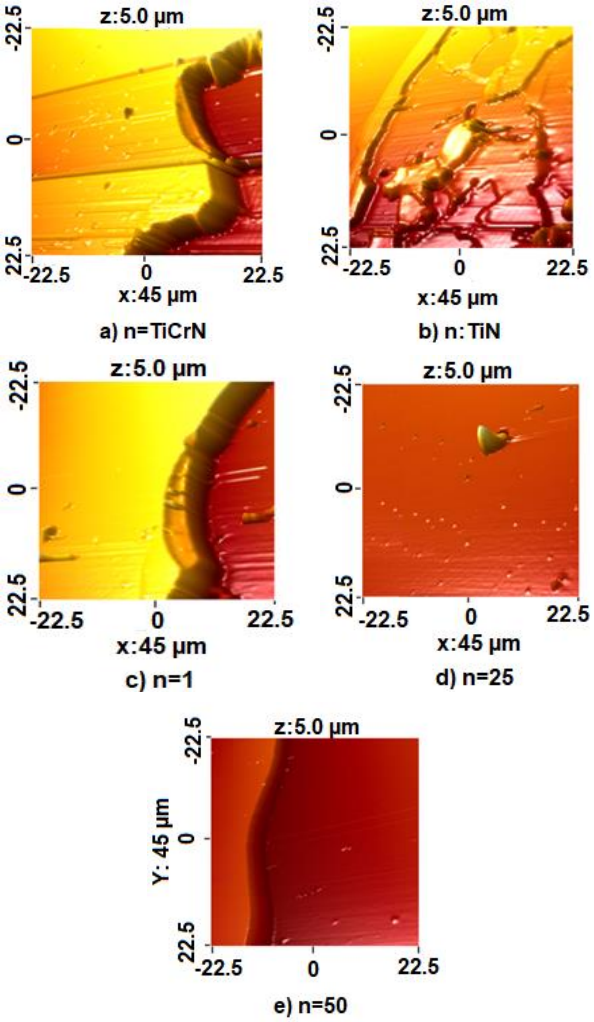

Fig. 4 Atomic force microscopy for monolayer and multilayer coatings (a) TiCrN (b) TiN (c) 1 bilayer (d) 25 bilayers and e) 50 bilayers.

The roughness decreased as the number of bilayers was increased as shown in Fig. 5a, because an increase in system density is promoted due to a greater number of interfaces. Authors such as J.C Caicedo et al. [13] also showed this behaviour in multilayers systems The roughness is a factor that influenced the tribological properties, influencing the formation of asperities, the type of contact and the wear generated at the beginning of the tribological test [15,14], thus, the coating with 50 bilayers presented a decrease in the formation of asperities, a greater area of contact and less wear at the beginning of the tribological test, as corroborated later in Fig. 9a. In addition, the coating with 50 bilayers presented an increase in the resistance to corrosion, as corroborated in the electrochemical properties obtained in this investigation, since this surface had a smaller amount of imperfections, roughness or a less irregular morphology which decreased the passage of the electrolyte to the substrate-coating interface [16], useful when incorporating liquid lubricants in the cutting processes for in the tools for which this coating is designed for.

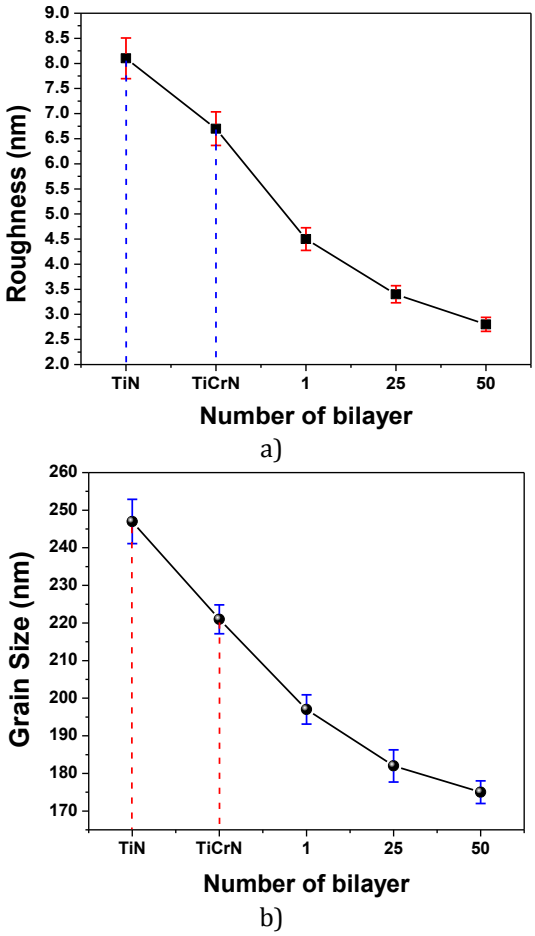

Fig. 5. a) Roughness for the monolayers (TiN and TiCrN) and multilayers [TiN/TiCrN]n as a function of the number of bilayers 1, 25 and 50; and b) Grain size for the monolayers (TiN and TiCrN) and multilayers [TiN/TiCrN]n as a function of the number of bilayers 1, 25 and 50.

Figure 5b shows the grain size versus the number of bilayers for the monolayer and multilayer coatings, where it could be seen that the grain size decreases as the number of bilayers increases due to nucleation effects, since the growth of the grains are interrupted when a new monolayer starts to be deposited and consequently, when many more layers are deposited, smaller grains start to form causing the microstructure to become more compact, much denser and giving rise to a lower roughness, as it is the case of the coating with the highest number of bilayers, as corroborated in Fig. 5a [13].

3.4 Mechanicals properties

Figure 6 shows the load-depth curves obtained during the nanoindentation test where it was observed that the highest penetration was obtained for the substrate (steel H13) and lower penetrations were obtained as the number of bilayers increased. This behaviour is due to the change of surface properties of each coating, mainly because there was an increase in the surface hardness as corroborated in Fig. 7a.

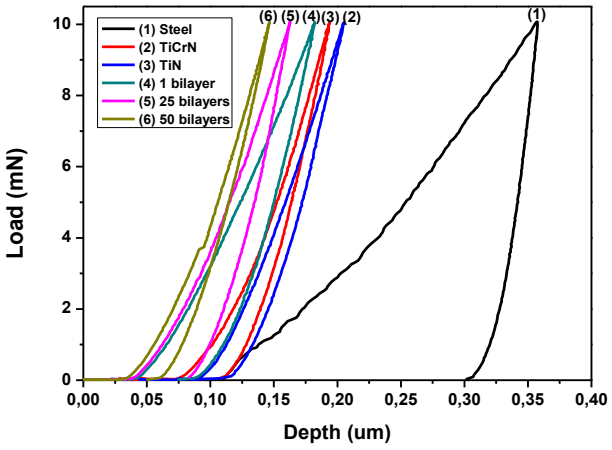

Fig. 6. Load-displacement curves for the monolayer (TiN and TiCrN) and multilayer [TiN/TiCrN]n systems as a function of the number of bilayers 1, 25 and 50.

Figures 7a and 7b show the values of hardness (H) and modulus of elasticity (E) for monolayer (TiN and TiCrN) and multilayers coatings where it was determined that the values obtained are greater than 10 Gpa except for the substrate (steel H13); This serves as a parameter to describe them as hard coatings, which allows to have a longer life time and lower wear rates in cutting tools that implement this type of coatings [17].

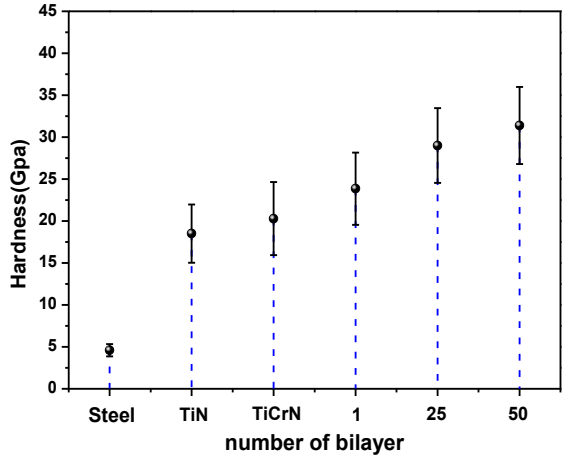

a)

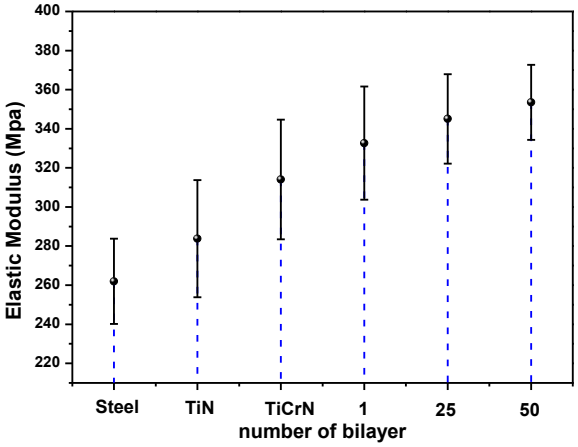

b)

Fig. 7. a) Hardness for the monolayers (TiN and TiCrN) and multilayers [TiN/TiCrN]n as a function of the number of bilayers 1, 25 and 50; and b) Modulus of elasticity for the monolayers (TiN and TiCrN) and multilayers [TiN/TiCrN]n as a function of the number of bilayers 1, 25 and 50.

A hardness of 18.5 Gpa and a modulus of elasticity 284.17 Mpa as well as a hardness of 20.35 Gpa and a modulus of elasticity of 314.20 Mpa were obtained for the monolayers of TiN and TiCrN respectively. The TiCrN monolayer showed betters properties due to greater compressive stresses that were generated in the coating during the sputtering of the deposition process [13]. For the multilayer coatings it was observed that the hardness increased according to the number of bilayers, where the highest hardness was 31.38 Gpa for the coating with 50 bilayers as shown in Fig. 7a [5]. Authors such as J.C Caicedo [13] and collaborators attributed this behaviour not only to the compressive stress during the deposition process but also to a physical order that is produced by the increase in the number of interfaces, which causes an impediment to the movement of dislocations, because a high density

of grain edge is promoted, causing the dislocations to slide through these interfaces, which requires a higher stress of critical creep related to the differences in the shear modulus of the materials [5]. Another aspect related to the change of properties such as hardness and modulus of elasticity, is due to the nanometric size of the grains, Z.B. Qi et al. [22] determined the inverse effect of the grain size in the hardness of the coatings stating that when originating much smaller grains, a greater density of grain boundary per unit volume is generated, causing a damming of the dislocations generated by an effort, hindering the crack propagation and thus increasing the hardness and modulus of elasticity of the coating; In this way, having a coating with a smaller grain size and with a greater number of interfaces such as the coating with 50 bilayers, will have better mechanical properties as corroborated in Figs. 7a and 7b [13,12].

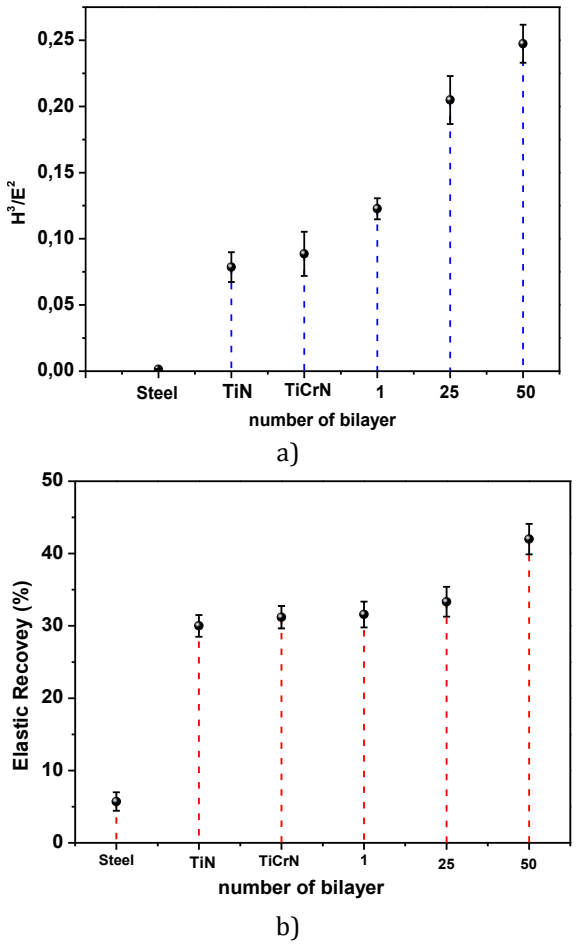

Fig. 8. a) Resistance to plastic deformation for mechanical properties for monolayers (TiN and TiCrN) and multilayers [TiN/TiCrN]n as a function of the number of bilayers 1, 25 and 50; and b) Elastic recovery for mechanical properties for monolayers (TiN and TiCrN) and multilayers [TiN/TiCrN]n as a function of the number of bilayers 1, 25 and 50.

From the results obtained by the nanoindentation test, other properties such as plastic deformation resistance (H^3/E^2) and elastic recovery were calculated, which are illustrated in Figs. 8a and 8b respectively. The elastic recovery was calculated from of Eq. 3:

$$R = \frac{\delta max - \delta p}{\delta max} \quad (3)$$

where δ_{max} is the maximum displacement and δp is the residual or plastic displacement. These data were obtained from the load-depth curve of the indentation test.

It was observed that the resistance to plastic deformation, as well as the elastic recovery increased as the number of bilayers did as well; This is due to the properties of such surfaces, as mentioned above, by increasing the number of interfaces, it decreases the grain size and increases the grain boundary density, causing an impediment to the movement of microcracks and thus making it difficult for the surface of the coating with fifty bilayers to be deformed, being able to withstand greater stresses [12].

3.5 Tribological Properties

3.5.1 Pin On Disk

Figure 9a shows the friction coefficient versus distance during the tribological test, where two representative stages can be seen. Stage I, known as the starting period, where there is a rapid increase in the friction coefficient due to the contact between the asperities and the annihilation of the same ones that exist between the two surfaces in contact, the counterpar (Steel 440) and the surface to be studied, followed by a stage of stabilization. Stage II, known as running-in, in which the annihilation of the asperities is maintained together with the appearance of defects of the coating, leading to the formation of wear particles or debris [15].

In Figure 9b a decrease in the friction coefficient can be observed as the number of bilayers increases. The above can be related to the proposed mechanical frictional model of Archard Eq. 4:

$$\mu = \frac{F_f}{F_n} = C_k \cdot \frac{R_{(s,a)}}{\sigma t_{(H,Er)}} \quad (4)$$

where μ is the coefficient of friction, C_k is a constant that depends on the parameters of the

test, $R_{(s,\,a)}$ is the roughness of the coating, and σt is a variable that takes into account the elastic-plastic properties (hardness, H, or elastic modulus, Er), obtained by mechanical measurements. According to this model, when the surface of the coating presents a low roughness (Fig. 5a) and a high hardness (Fig. 7a) the coefficient of friction will be lower, therefore, the coating with 50 bilayers would have a lower friction coefficient in comparison to other surfaces [12].

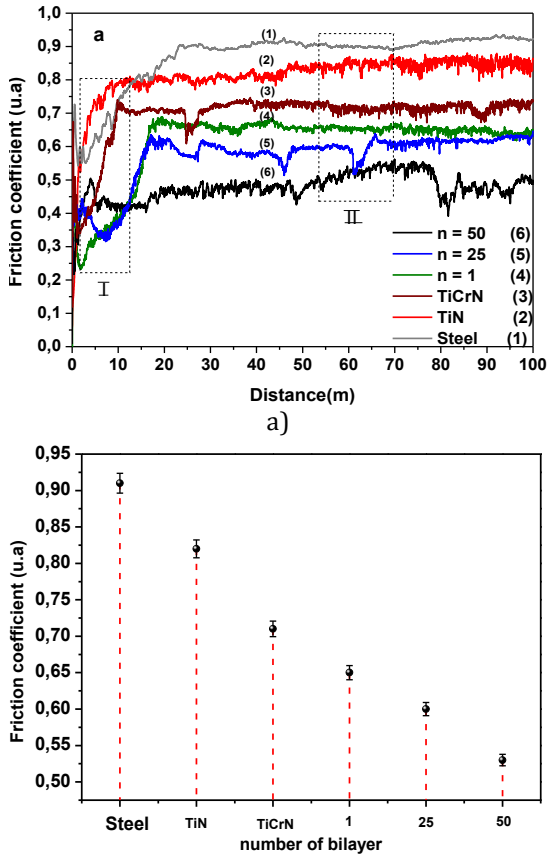

a)

b)

Fig. 9. a) Friction coefficient for the monolayers [TiN and TiCrN] and multilayers [TiN/TiCrN]n as a function of the number of bilayers 1, 25 and 50; and b) Reduction of the friction coefficient for the monolayers [TiN and TiCrN] and multilayers [TiN/TiCrN]n as a function of the number of bilayers 1, 25 and 50.

Figure 10 shows the micrographs of the wear tracks generated in the pin on disk test, for the substrate, the monolayer and multilayer coatings, where several wear mechanisms (abrasive, plowing, adhesion and fatigue) could be seen. In the case of abrasive wear, it was produced by the annihilation of the asperities by the continuous passage of the counterpart on the surface to be studied, generating abrasive particles which are plastically deformed and hardened during the tribological test, these particles adhere to both surfaces (counterpar and coating) generating plowing on the surface; The adhesive wear occurred because in certain areas the coating was able to withstand the external load exerted by the counterpar [15].

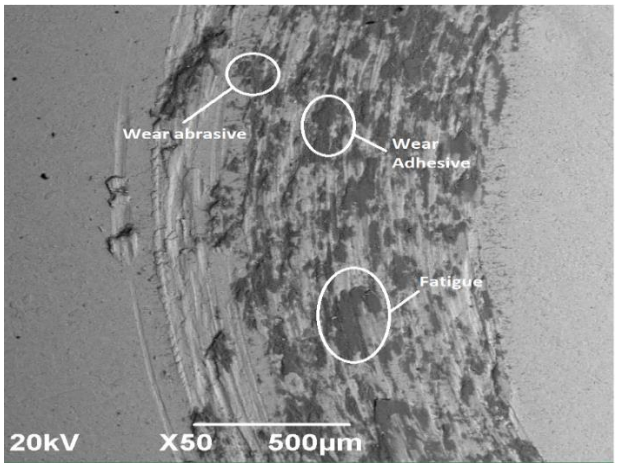

a) Steel

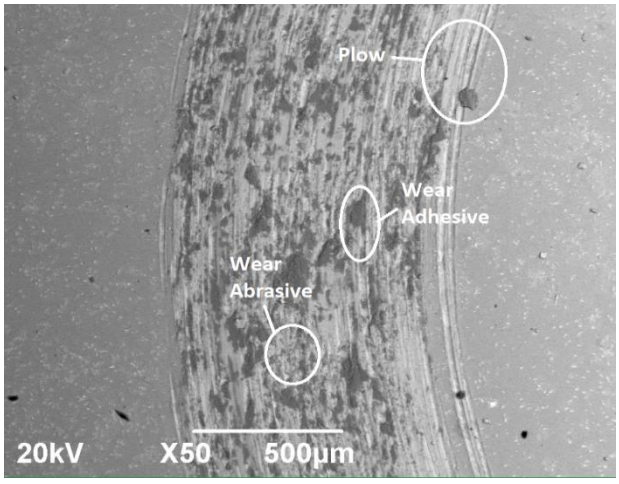

b) TiN

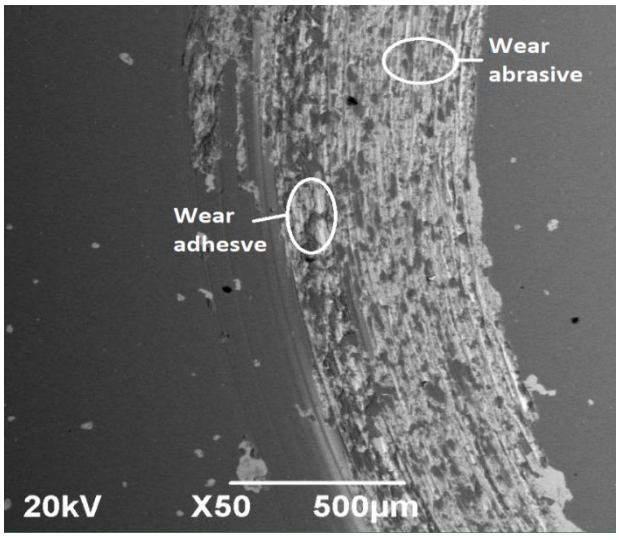

c) TiCrN

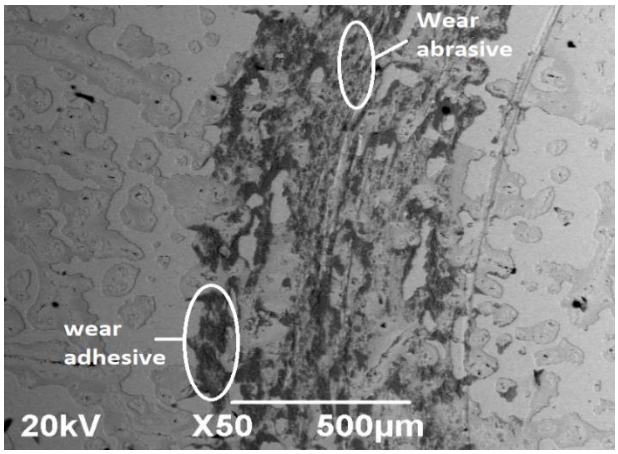

d) 1 bilayer

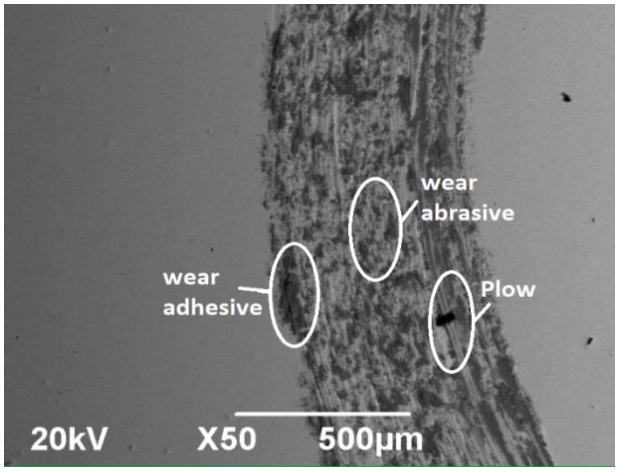

e) 25 bilayer

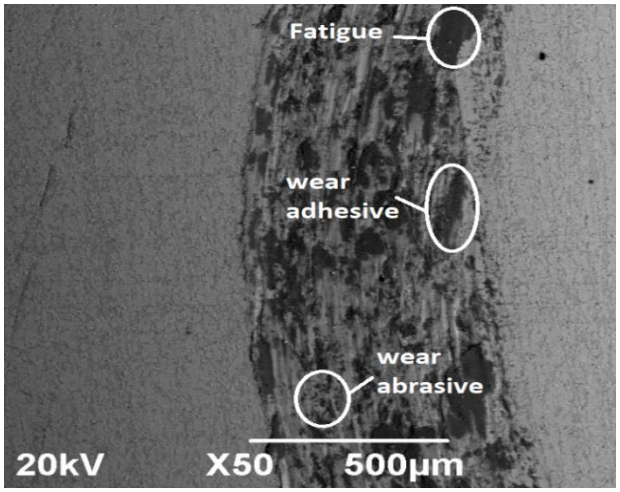

f) 50 bilayers

Fig. 10. SEM micrograph of the wear tracks produced by the tribological tests at a resolution of x50.

In the micrographs it can be seen that for the substrate (Steel H13) and the monolayer coatings (TiN and TiCrN), respectively, in Figs. 10a, 10b and 10c the wear mechanism that predominates was abrasive wear which produced a plow over surface, due to its low hardness and high roughness, therefore, these surfaces had a low resistance to plastic deformation; Due to this, a large number of particles were produced on the surface which deformed it throughout the tribological test, producing a "scratched it" on the surface. For multilayer coatings and as proposed by authors such as WF Piedrahita and collaborators [15] it was evident that the predominant mechanism was an adhesive type wear and when the number of bilayers increased, as was the case with the coating with 50 bilayers, shown in Fig. 10f, this mechanism was much more evident because these surfaces had better properties, such as higher hardness, higher resistance to plastic deformation and a low roughness, causing the surface for this coating to be able to withstand the interaction of the counterpar decreasing the amount of particles produced on its surface and increasing its life time.

3.5.2 Tribological Properties "Dynamic scratching"

The scratch test was used to characterize the adherence of the coatings. The adhesion property of a coating can be characterized mainly by Lc1, which is known as the cohesive failure where it begins to produce the first cracks or first faults on the coating and Lc2 known as the adhesive failure where a delamination occurs in the edge of the track line.

Figure 11 shows the adhesion strength for the monolayer and multilayer coatings as a function of the Lc1 and Lc2 faults, where slope changes corresponding to the adhesive and cohesive failure were observed, corroborating with the micrographs of the wear tracks for each test where the morphological changes suffered by the surface due to cohesive and adhesive failure are appreciated (Fig. 12) [18].

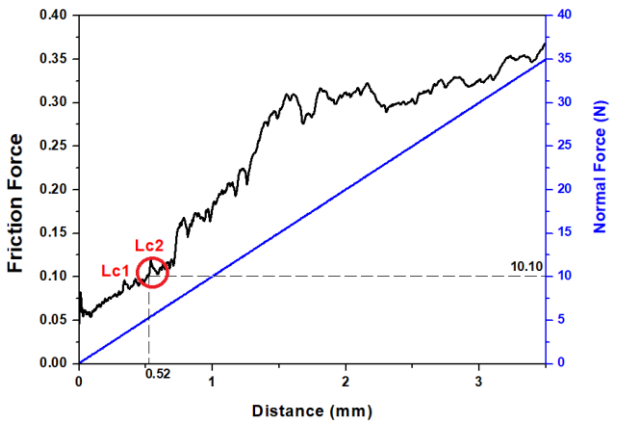

a) TiN

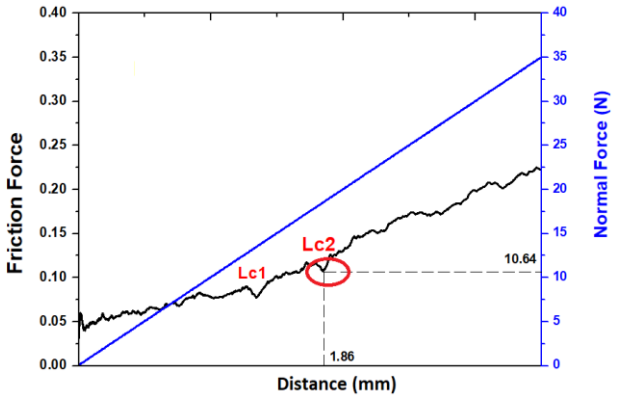

b) TiCrN

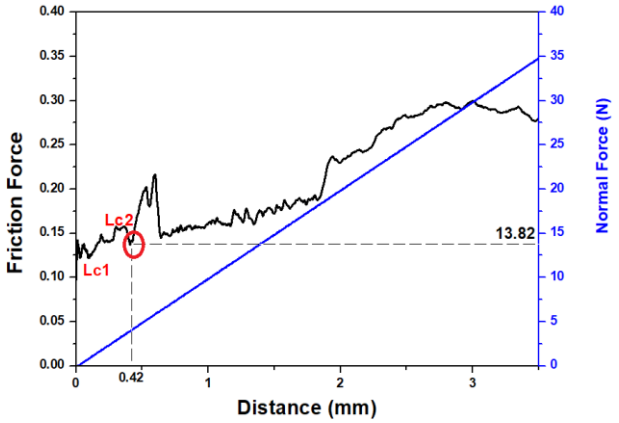

c) 1 bilayer

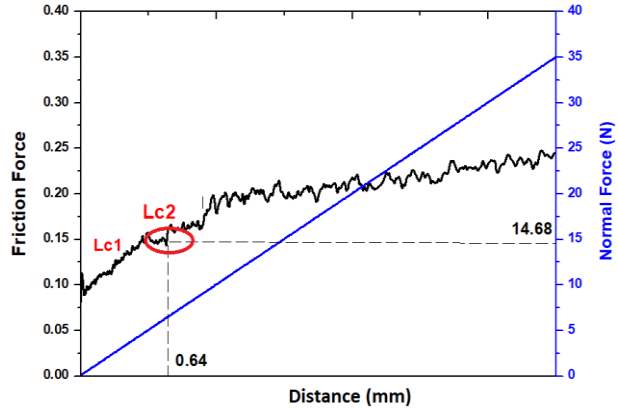

d) 25 bilayer

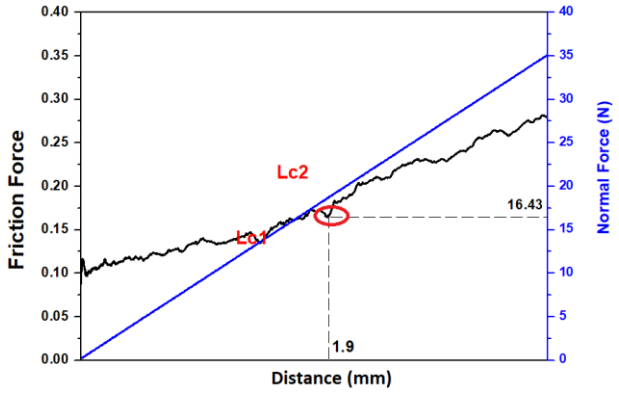

e) 50 bilayer

Fig. 11. Friction coefficient and normal strength versus distance.

Figure 12 presents the images of optical microscopy of the scratching tracks during the test where the cohesive and adhesive failures were located for all the systems. It was found that when the number of bilayers was increased both the cohesive and adhesive failures were found at higher distances from the beginning of the test, the reason for this is that by increasing the number of interfaces the surface has a greater resistance to being deformed as corroborated in Fig. 8a, thus avoiding the presence of faults and increasing the adhesion strength of the system.

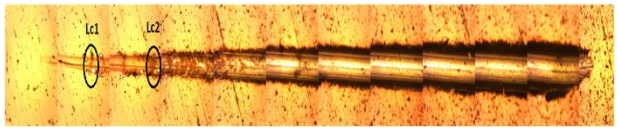

a) TiN

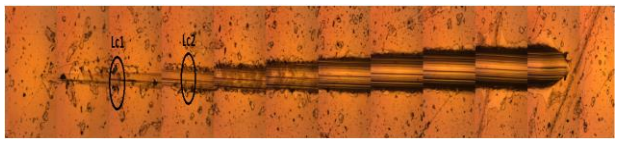

b) TiCrN

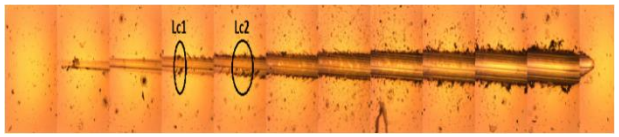

c) 1 bilayer

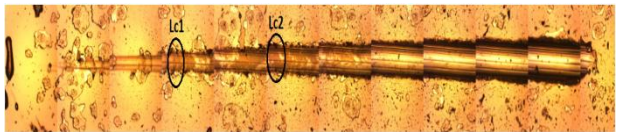

d) 25 bilayer

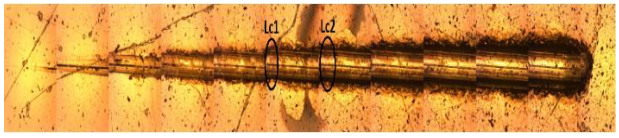

e) 50 bilayer

Fig. 12. Optical micrographs of the wear track of the dynamic scratch test at a resolution of x10.

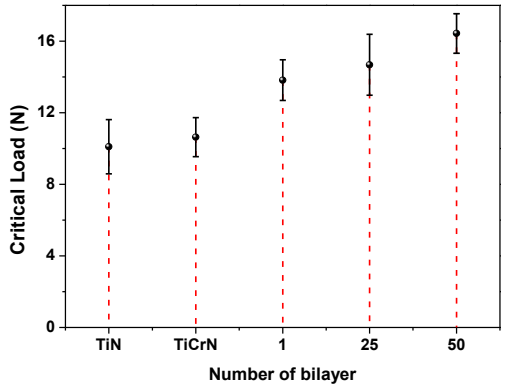

Fig. 13. Critical load Lc2 for monolayers (TiN and TiCrN) and multilayers [TiN/TiCrN]n as a function of the number of bilayers 1, 25 and 50.

Figure 13 shows the behavior of the adhesive failure "Lc2" where it was observed that the critical load increased as the number of bilayers did as well. Thus, the highest critical load was obtained for the coating with 50 bilayers due to an increase in adhesion energy of the system, since a greater number of interfaces allows an attenuation of the energy transferred by the applied external load also the existence of multiple interfaces and grain boundaries that block the growth and advancement of microcracks that are formed during scratching, improving the adherence of the coating [19].

3.6 Electrochemical Properties

3.6.1 Electrochemical properties: Electrochemical impedance (EIS)

Figure 14 shows the Nyquist diagram for all systems, where an increase in the radius of the semicircles was seen as the number of bilayers increased. This fact indicates that the time it takes for the Cl-- ions present in the electrolyte (NaCl + H2O) to cross through the entire coating until reaching the substrate is greater [20] because a greater number of interfaces generates a much denser structure causing a greater obstacle to the passage of the electrolyte.

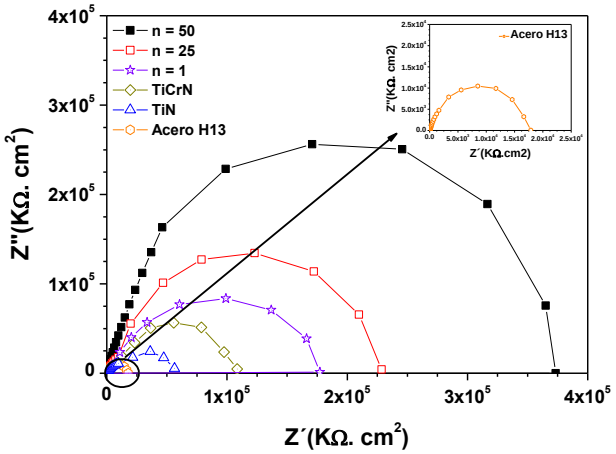

Fig. 14. Nyquist diagram for monolayer (TiN and TiCrN) and multilayer [TiN/TiCrN]n coatings as a function of the number of bilayers 1, 25 and 50.

Figure 15 shows the polarization resistance of the studied materials. Here it is seen that as the number of bilayers increased, the resistance to polarization also increased. This resistance is inversely proportional to the corrosion rate, which means that the increase of bilayer number created a decrease in corrosion rate, as corroborated in Figure 18 which shows the corrosion rate for all the systems studied. With this, it was determined that the system with 50 bilayers, showed a greater resistance to polarization and therefore a lower corrosion rate.

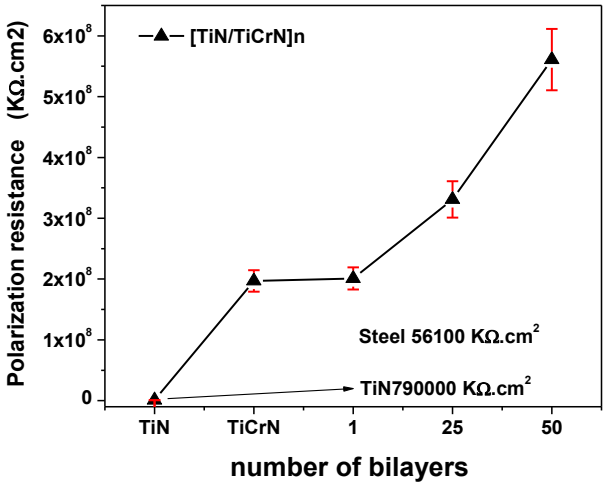

Fig. 15. Polarization resistance for monolayers (TiN and TiCrN) and multilayers [TiN/TiCrN]n as a function of the number of bilayers 1, 25 and 50.

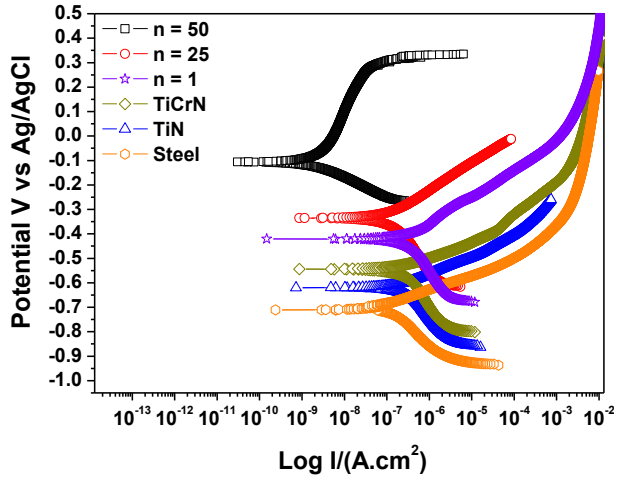

Fig. 16. Tafel curves for monolayers (TiN and TiCrN) and multilayers [TiN/TiCrN]n as a function of the number of bilayers 1, 25 and 50.

Figure 16 shows the tafel curves for all the systems, where it was evident that when the coatings were incorporated over the substrate, the curves moved towards the upper areas of the graph "more electropositive potential" and to the left "areas of lower density ", confirming the protective effects of the coatings. This behaviour is reflected mainly by increasing the number of bilayers, authors such as C. Escobar and colleagues [20] concluded that this characteristics in multilayer coatings is due to the fact that when the number of interfaces increases, the system

becomes much denser, it decreasing the irregularity in the surface as well as the presence of pores, hindering the passage of the Cl- ion towards the substrate, and generating a better protection against aggressive environments.

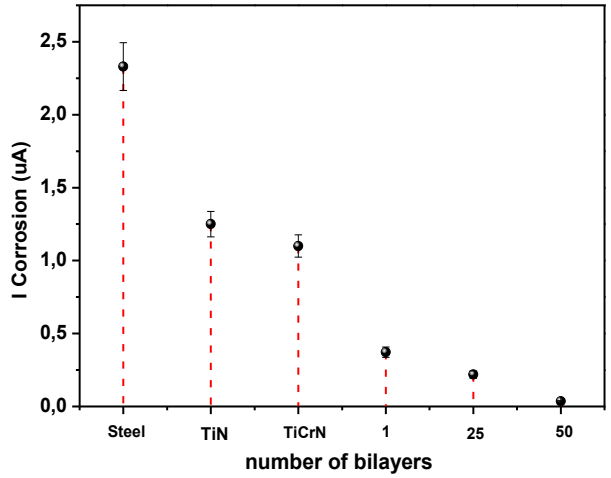

Fig. 17. Corrosion current for the substrate, monolayers (TiN and TiCrN) and multilayers [TiN/TiCrN]n as a function of the number of bilayers 1, 25 and 50.

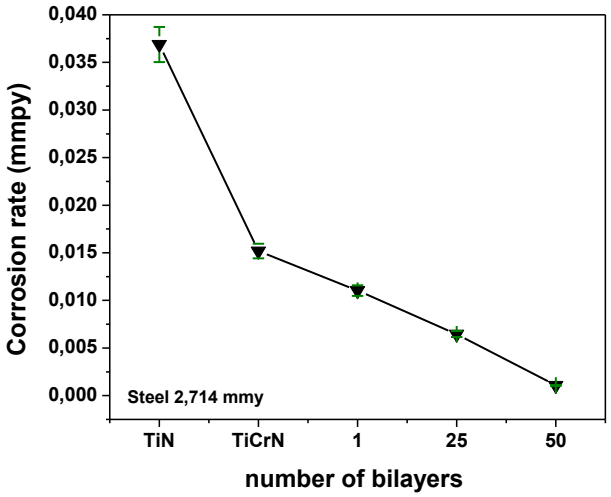

Fig. 18. Corrosion rate for the substrate (steel H13), monolayers (TiN and TiCrN) and multilayers [TiN/TiCrN]n as a function of the number of bilayers 1, 25 and 50.

Figure 17 shows the corrosion current as a function of the number of bilayers, which was calculated from Eq. 5, where it was observed that by increasing the number of bilayers the corrosion current presented a decrease due to the fact that increasing the number of interfaces promotes a greater amount of barrier to the passage of electrolyte to the substrate. Thus, making a direct attack of the chlorine ion Cl- on the surface difficult [16,21], therefore, the system with 50 bilayers had a lower corrosion current compared to the other systems.

$$I_{corr} = \frac{\beta a \beta c}{2.303 Rp\ (\beta a + \beta c)} \quad (5)$$

$$Corrrrosion\ rate = \frac{i_{corr} * K * E_W}{d} \quad (6)$$

Figure 18 shows the corrosion rate (mm / y) versus the number of bilayers. The corrosion rate was calculated from Eq.6, corroborating the results obtained by the tafel curves in Figure 16 where it was proven that by increasing the number of interfaces or breaking of symmetry, a greater protection against corrosive media is generated due to a greater number of barriers that prevent the passage of electrolyte to the substrate; consequently, the lowest corrosion rate was presented by the system with the greater number of bilayers (50).

4. MERIT INDEX

After carrying out the respective characterizations of the multilayer coatings [TiN/TiCrN]n the index of merit was performed, which relates properties that are not comparable with the objective of finding the optimum point where multilayer coatings have the best properties.

Figure 19a shows the index of merit that relates the properties of hardness versus the resistance to polarization as a function of the number of bilayers. It is seen that both properties increased as the number of bilayers did as well, concluding that the best properties were obtained for the coating with 50 bilayers.

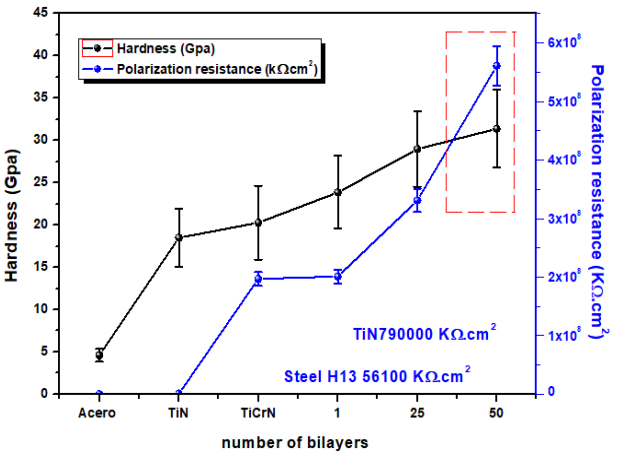

a)

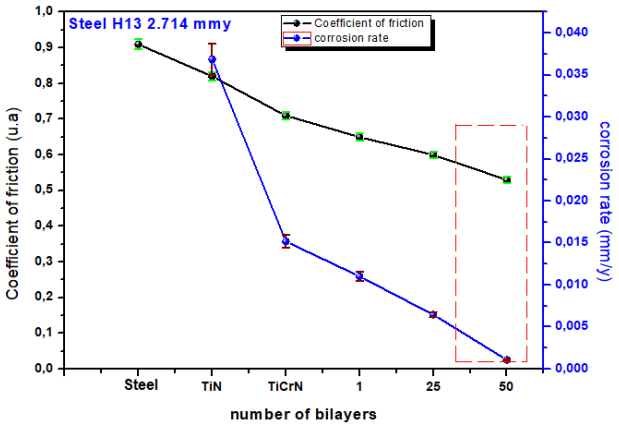

b)

Fig. 19. Merit index for: a) hardness versus polarization resistance, b) coefficient of friction versus corrosion rate.

Figure 19b shows the index of merit for the coefficient of friction versus the corrosion rate, where it was determined that both properties decreased as the number of bilayers increased, leaving clear that the point where the best features are present is at the coating with 50 bilayers.

With the previous data, it can be established that the multilayer coating with 50 bilayers presented a better set of mechanical, tribological and electrochemical properties when compared to the others, making this system ideal when coating cutting tools, prolonging their service life.

5. CONCLUSIONS

The monolayer (TiN and TiCrN) and multilayer coatings [TiN / TiCrN] n showed face centered cubic crystal structure (FCC); The incorporation of Cr in the crystal structure of TiN caused a compressive type deformation in its structure; Also an increase the number of bilayers produced an increase in this deformation, obtaining a more dense, compact structure with a smaller grain size, causing a more regular surface and decreasing the surface roughness.

The mechanical and tribological properties increased as the number of bilayers also increased, since increasing the number of interfaces generated greater obstacles to the dislocation movement, requiring a greater amount of energy for these dislocations to overcome said obstacles, causing the surface to have a higher hardness, modulus of elasticity, greater resistance to deformation and less surface wear.

By having a greater number of obstacles due to a greater number of bilayers, the passage and velocity of the Cl- ion towards the substrate is diminished, decreasing the corrosion rate of the system and causing greater resistance to corrosion in aggressive environments.

By means of the index of merit, the coherent synergism between the mechanical, tribological and electrochemical properties was shown as a function of the number of bilayers, which evidenced that the coating with 50 bilayers presented the best set of properties, determining that this coating is the best option to be incorporated on cutting tools.

Acknowledgement

This study was supported by " Vicerrectoría de Investigaciones de la Universidad del Valle" project number C.I 71159 and by "Vicerrectoría de Investigaciones de la Universidad Militar Nueva Granada" project number ING-2992, validity 2019, as well as the researchs groups "Laboratorio de Recubrimientos Duros y Aplicaciones Industriales" and "Metalurgia Física y Teoría de Transiciones de Fase" from the "Universidad del Valle".

REFERENCES

[1] D.D. Kumar, N. Kumar, S. Kalaiselvam, S. Dash, R. Jayavel, *Wear resistant super-hard multilayer transition metal-nitride coatings*, Surfaces and Interfaces, vol. 7, pp. 74–82, 2017, doi: 10.1016/j.surfin.2017.03.001

[2] F.S. Osorio, J.A. Trujillo, M. Benavides, G.B. Gaitán, *Propiedades mecánicas y tribológicas de recubrimientos duros: Uso de la técnica de nanoindentación*, Informador Técnico, vol. 65, pp. 38-46, 2002, doi: 10.23850/22565035.898

[3] V. Prabakaran, K. Chandrasekaran, *Characterisation and Corrosion Resistance of TiCrN Composite Coating on Steel by Physical Vapour Deposition Method*, Journal of Bio- and Tribo-Corrosion, vol. 2, no. 4, pp. 1–6, 2016, doi: 10.1007/s40735-016-0055-y

[4] H. Zhang, Z. Li, W. He, B. Liao, G. He, X. Cao, Y. Li, *Damage evolution and mechanism of TiN/Ti*

multilayer coatings in sand erosion condition, Surface and Coatings Technology, vol. 353, pp. 210–220, 2018, doi: 10.1016/j.surfcoat.2018.08.062

[5] G. Pradhaban, P. Kuppusami, D. Ramachandran, K. Viswanathan, R. Ramaseshan, *Nanomechanical properties of TiN/ZrN multilayers prepared by pulsed laser deposition*, MaterialsToday: Proceedings, vol. 3, iss. 6, pp. 1627–1632, 2016, doi: 10.1016/j.matpr.2016.04.052

[6] J.C. Caicedo, A. Guerrero, W. Aperador, *Determination of multilayer effect evidence on metal carbon-nitride system*, Journal of Alloys Compounds, vol. 785, pp. 178–190, 2019, doi: 10.1016/j.jallcom.2019.01.151

[7] Z. Geng, G. Shi, T. Shao, Y. Liu, D. Duan, T. Reddyhoff, *Tribological behavior of patterned TiAlN coatings at elevated temperatures*, Surface and Coatings Technology, vol. 364, pp. 99–114, 2019, doi: 10.1016/j.surfcoat.2019.02.076

[8] H. Li, C. Zhang, C. Liu, M. Huang, *Improvement in corrosion resistance of CrN coatings*, Surface and Coatings Technology, vol. 365, pp. 158–163, 2019, doi: 10.1016/j.surfcoat.2018.07.018

[9] E. Silva, M. Rebelo de Figueiredo, R. Franz, R.E. Galindo, C. Palacio, A. Espinosa, S.V. Calderon, C. Mitterer, S. Carvalho, *Structure-property relations in ZrCN coatings for tribological applications*, Surface and Coatings Technology, vol. 205, iss. 7, pp. 2134–2141, 2010, doi: 10.1016/j.surfcoat.2010.08.126

[10] V.V.A. Thampi, A. Bendavid, B. Subramanian, *Nanostructured TiCrN thin films by Pulsed Magnetron Sputtering for cutting tool applications*, Ceramics International, vol. 42, iss. 8, pp. 9940–9948, 2016, doi: 10.1016/j.ceramint.2016.03.095

[11] W. Aperador, A. Delgado, J.C. Caicedo, *Analysis of corrosion degradation of TiCrN coatings subjected to high temperatures*, Interantional Journal of Electrochemical Science, vol. 12, pp. 4502–4514, 2017, doi: 10.20964/2017.05.33

[12] L. Ipaz, J.C. Caicedo, J. Esteve, F.J. Espinoza-Beltran, G. Zambrano, *Improvement of mechanical and tribological properties in steel surfaces by using titanium-aluminum/titanium-aluminum nitride multilayered system*, Applied Surface Science, vol. 258, iss. 8, pp. 3805–3814, 2012, doi: 10.1016/j.apsusc.2011.12.033

[13] J.C. Caicedo, G. Cabrera, H.H. Caicedo, C. Amaya, W. Aperador, *Nature in corrosion-erosion surface for [TiN/TiAlN]n nanometric multilayers growth on AISI 1045 steel*, Thin Solid Films, vol. 520, iss. 13, pp. 4350–4361, 2012, doi: 10.1016/j.tsf.2012.02.061

[14] J.H. Navarro-Devia, C. Amaya, J.C. Caicedo, W. Aperador, *Performance evaluation of HSS cutting tool coated with hafnium and vanadium nitride multilayers, by temperature measurement and surface inspection, on machining AISI 1020 steel*, Surface and Coatings Technology, vol. 332, pp. 484–493, 2017, doi: 10.1016/j.surfcoat.2017.08.074

[15] W.F. Piedrahita, W. Aperador, J.C. Caicedo, P. Prieto, *Evolution of physical properties in hafnium carbonitride thin films*, Journal of Alloys and Compounds, vol. 690, pp. 485–496, 2017, doi: 10.1016/j.jallcom.2016.08.109

[16] W. Aperador, P. Prieto, C. Escobar, H.H. Caicedo, M. Villarreal, J.C. Caicedo, *Diagnostic of corrosion–erosion evolution for [Hf-Nitrides/V-Nitrides]n structures*, Thin Solid Films, vol. 545, pp. 194–199, 2013, doi: 10.1016/j.tsf.2013.07.081

[17] C. Donnet, A. Erdemir, *Historical developments and new trends in tribological and solid lubricant coatings*, Surface and Coatings Technology, vol. 180-181, pp. 76–84, 2004, doi: 10.1016/j.s.urfcoat.2003.10.022

[18] J.C. Caicedo, W. Aperador, C. Amaya, *Determination of physical characteristic in vanadium carbon nitride coatings on machining tools*, The International Journal of Advanced Manufacturing Technology, vol. 91, iss. 1–4, pp. 1227–1241, 2017, doi: 10.1007/s00170-016-9835-2

[19] J.M. Saldaña, J.C. Caicedo, G. Cabrera, P. Prieto, L. Yate, C. Amaya, *Enhancement of mechanical and tribological properties in AISI D3 steel substrates by using a non-isostructural CrN/AlN multilayer coating*, Materials Chemistry and Physics, vol. 125, iss. 3, pp. 576–586, 2011, doi: 10.1016/j.matchemphys.2010.10.014

[20] C.A. Escobar, J.C. Caicedo, W. Aperador, *Corrosion resistant surface for vanadium nitride and hafnium nitride layers as function of grain size*, Journal of Physics Chemistry of Solids, vol. 75, iss. 1, pp. 23–30, 2014, doi: 10.1016/j.jp.cs.2013.07.024

[21] J.C. Caicedo, G. Cabrera, W. Aperador, H.H. Caicedo, A. Mejia, *Determination of the best behavior among AISI D3 steel, 304 stainless steel and CrN/AlN coatings under erosive-corrosive effect*, Vacuum, vol. 86, iss. 12, pp. 1886–1894, 2012, doi: 10.1016/j.vacuum.2012.05.007

[22] Z.B Qi, P Sun, F.P Zhu, Z.C Wang, D.L Peng, C.H Wu, *The inverse Hall-Petch effect in nanocrystalline ZrN coatings*, Surface and Coatings Technology, vol. 205, iss. 12, pp. 3692–3697, 2011, doi: 10.1016/j.surfcoat.2011.01.021